Common-mode Inductor Saturation Analysis and Design Optimization Based on Spectrum Concept

Ruirui Chen[1], Zheyu Zhang[1], Ren Ren[1], Jiahao Niu[1], Handong Gui[1], Fred Wang[1,2], Leon M. Tolbert[1,2], Daniel J. Costinett[1,2] and Benjamin J. Blalock[1]

[1]Department of Electrical Engineering and Computer Science, The University of Tennessee, Knoxville, TN, USA

[2]Oak Ridge National Laboratory, Knoxville, TN, USA

rchen14@vols.utk.edu

***Abstract*—Understanding the CM inductor core saturation mechanism and reducing core flux density is critical for CM inductor design optimization. Instead of a time domain method, this paper introduces frequency domain spectrum concept for CM inductor core saturation analysis and design optimization, which will provide designers a better understanding of CM inductor design. First, both core permeability and converter modulation index's opposite influence on DM flux density and CM flux density are identified. Then, CM flux density is further investigated based on the spectrum concept. Three components in the CM inductor which may cause large CM flux density and core saturation are summarized: (1) switching frequency related components, (2) impedance resonance frequency related components, and (3) modulation frequency related components. Each component is investigated for CM flux density reduction and filter design optimization. A connecting AC and DC side midpoint with notch filter structure is proposed to reduce modulation frequency related components. Experiment results are presented to verify the proposed concept and method.**

Keywords—Common-mode inductor; EMI filter design; core saturation; EMI spectrum.

I. INTRODUCTION

The switching action of power electronic devices generate electromagnetic interference (EMI) noise. To attenuate the EMI noise emissions and satisfy electromagnetic compatibility (EMC) standards, EMI filters are employed in power converter systems. However, these passive filters such as the common-mode (CM) inductors usually take a large portion of total weight and volume of the converter system, especially in electric vehicles and aircrafts applications. EMI filters weight and volume reduction is critical to increase converter system power density.

In CM inductor design, core saturation is one of the main limitations for inductor weight reduction. Overdesign of the inductor core is a safe way to prevent saturation, but it will decrease the converter system power density. The mechanism of core saturation is complicated. As presented in [1] and [2], core saturation can be caused by the leakage flux associated with differential-mode (DM) current. In [3], the DM current excitation is considered as the main factor causing saturation. This may be true in some applications. However, in many other cases, the CM current produced flux can also cause core saturation. In [4], core saturation due to CM noise propagation path resonance is illustrated. And in [4] - [7], CM voltage is investigated to estimate the CM current in motor drives. Thus, both DM flux density and CM flux density need to be considered for core saturation analysis. However, in previous work, system parameters' different influence on DM and CM flux density and how these will influence filter design are not illustrated. Moreover, the mechanisms which may cause large CM flux density and lead to core saturation have not been fully identified and developed. In terms of CM filter design, a practical design procedure is proposed in [15]. CM filter design considering system impedance and filter parasitics is presented in [21]. CM filter design optimization considering converter switching frequency and corresponding impact on the filter is illustrated in [22]. In previous work, the influence of different frequency domain spectrum components on inductors and inductor design optimization from spectrum perspective are not clearly illustrated.

This paper presents comprehensive understanding and analysis on the CM inductor saturation mechanism and design optimization based on spectrum concept. Considering both DM flux density and CM flux density, it is shown that both magnetic core permeability and converter modulation index have opposite influence on CM flux density and DM flux density. CM flux density is further investigated based on spectrum concept. Three components in a CM inductor which may cause large CM flux density and lead to core saturation are summarized. Each component is discussed in detail to reduce CM flux density, avoid saturation and optimize filter design. A connecting AC and DC midpoint with notch filter structure is proposed to suppress the modulation frequency related components in the CM inductor. Experiment results are presented to verify the proposed concept and method.

II. DM AND CM FLUX DENSITY ANALYSIS

DM current generates magnetic field and flux in the CM inductor magnetic core. Most of this DM current generated flux of different phases cancel with each other in a balanced system. However, part of the DM flux of different phases which are not coupled will not be cancelled with each other (which is known as the leakage flux). The CM voltage of a converter will generate CM current through the impedance loop formed by system parasitics to the ground. This CM current will also generate flux in the core. Hence, the flux density in a CM inductor core can be divided to two parts.

$$B = B_{CM} + B_{DM} \tag{1}$$

where B_{CM} and B_{DM} are the CM current generated flux density and DM current generated flux density of the leakage inductance, respectively.

The CM and DM flux density can be expressed as

$$B_{CM} = \frac{\mu_0 \mu_r N \cdot 3I_{cm}}{L_e} \tag{2}$$

$$B_{DM} = \frac{\mu_0 \mu_{dm} N \cdot I_{dm}}{L_{eff}} \tag{3}$$

where μ_o and μ_r are the free space permeability and relative permeability, N is the number of turns, L_e is the mean path length, μ_{dm} is the equivalent leakage flux path relative permeability and L_{eff} is the equivalent leakage flux mean path length, respectively. The calculation of μ_{dm} and L_{eff} are developed in [8] and will not be repeated here.

The number of turns N and CM flux density B_{CM} can be represented by the required CM inductance L_{cm}.

$$N = \sqrt{\frac{L_{cm} L_e}{\mu_0 \mu_r A_e}} \tag{4}$$

$$B_{CM} = \sqrt{\frac{L_{cm} \mu_0 \mu_r}{A_e L_e}} \tag{5}$$

An evaluate of the influence of permeability and modulation index on inductor core flux density is conducted. First, when permeability μ_r increases, N decreases with the given L_{cm} as shown in (4). Therefore, B_{DM} decreases as shown in (3) while B_{CM} increases as shown in (5). Hence, permeability affects CM and DM flux density in opposite ways. It indicates that there is an optimal permeability μ_r to achieve minimum total flux density B. For CM filter design, different magnetic core materials need to be considered. Higher permeability material does not necessarily lead to smaller core size. Second, when a modulation scheme is determined, modulation index will influence the magnitude of the CM voltage. Take a two-level inverter as an example, with a lower modulation index, CM volt-second is larger which leads to larger CM current I_{cm}. However, lower modulation index means the output fundamental voltage and DM current I_{dm} are smaller. Hence, modulation index affects CM and DM current/flux density in opposite ways. Thereby, the worst operating condition for core flux density may not happen at full power (i.e., maximum modulation index). For CM filter design, the worst operating condition at the modulation index associated with maximum flux density needs to be identified to avoid core saturation.

III. CM Flux Density Analysis and Inductor Design Optimization based on Spectrum Concept

This section discusses mechanisms causing excessive CM flux density and illustrates CM inductor design optimization based on frequency domain spectrum concept. For a CM inductor, when the inductance is fixed, the CM volt-second or CM current will determine CM flux density as (6).

$$B_{CM} = \frac{\int V_{cm} dt}{NA_e} = \frac{\mu_0 \mu_r N \cdot 3I_{CM}}{L_e} \tag{6}$$

Next, an investigation the CM current existes in a CM inductor is done. Instead of time domain CM current, frequency domain spectrum concept is applied to CM current to provide an insightful view. A typical CM inductor CM current spectrum is shown in Fig. 1. The components in the current spectrum can be classified into three categories: 1) switching frequency related components; 2) impedance resonance frequency related components; and 3) modulation frequency related components. To reduce the CM flux density and optimize CM inductor design, each component in the inductor CM current spectrum needs to be reduced.

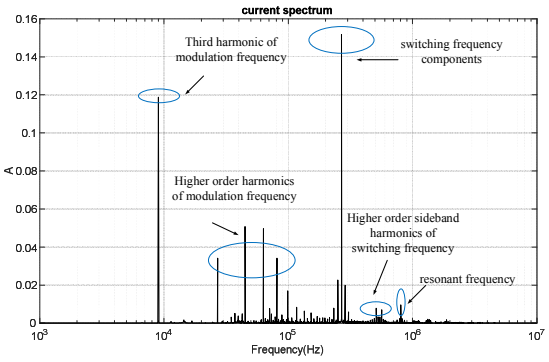

Fig. 1. CM inductor CM current spectrum.

The switching frequency related current components refer to switching frequency component and its sideband harmonics. The magnitudes of these components are determined by switching frequency related CM voltage and CM noise propagation path impedance. The CM noise propagation path impedance will be discussed later. To reduce switching frequency related CM voltage, pulse width modulation (PWM) schemes which reduce CM voltage amplitude can be applied such as the active zero state PWM (AZSPWM) and near state PWM (NSPWM) for two-level inverter [9] – [11], and common-mode reduction (CMR) scheme for three-level inverter [12]. Another method is to use variable switching frequency [13] [14], which spreads the centralized noise peak around the switching frequency and its multiples to a wider frequency range and thus reduces the CM voltage peak.

The impedance resonance frequency related current components are introduced by LC filter resonance, LC filter parasitics resonance, and load resonance. If the impedance resonance frequencies are close to the peak points of the CM voltage spectrum, the CM current will be amplified due to the relatively low impedance at these frequency points. LC filter corner frequency is determined by the required EMI noise attenuation obtained from the comparison of bare noise and EMI standard [15]. If the designed LC filter corner frequency f_{res} is higher than switching frequency f_{sw}, which usually occurs when f_{sw} is below the EMI frequency range and the switching frequency multiples determine the LC filter corner frequency,

then it is possible that the current will be amplified at certain multiples of f_{sw}. For example, as shown in Fig. 2, the LC filter corner frequency f_{res} is determined by the noise peak at switching frequency multiple $n2 * f_{sw}$, but another switching frequency multiple $n1 * f_{sw}$ is very close to the resonance point. Then CM current can be amplified and even cause core saturation. Hence, LC filter damping is necessary to avoid overdesign of the inductor. Load resonance can also cause large CM current and flux density. This excess CM current can be reflected in the EMI current bare noise spectrum. In this case, following the design procedure in [15], the LC filter corner frequency may be determined by the noise peak at resonance frequency instead of switching frequency or its multiples. This is not desired for an optimal design [20]. It is better to first damp this load resonance and then measure EMI bare noise and then determine the LC filter corner frequency. LC filter parasitics resonance involves filter parasitics or the coupling effect between multi-stage filters. In this case, it is suggested to check the EMI noise spectrum peak points after the EMI filter is added. If certain noise peaks are identified to be caused by impedance resonance, then damping networks can be considered.

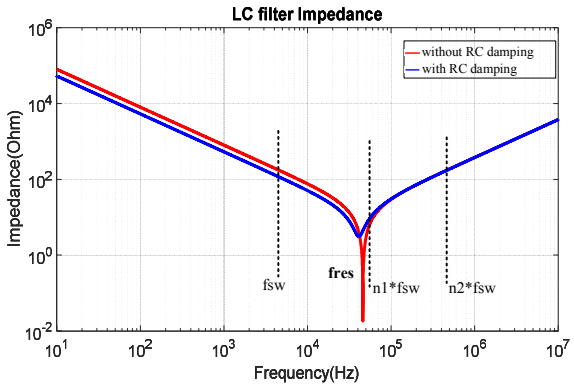

Fig. 2. LC filter corner frequency position and damping.

A Rd-Cd damping network can be employed for impedance resonance discussed above. For the optimal damping [16], $R_d = R_0\sqrt{\frac{(2+n)(4+3n)}{2n^2(4+n)}}$,where $R_0 = \sqrt{\frac{L}{C}}, n = \frac{C_d}{C}$.

The modulation frequency related components refer to the third, ninth or higher order harmonics of the fundamental component. Space vector modulation (SVM) is widely used in three phase converters to improve DC voltage utilization. However, this modulation method introduces low frequency modulation frequency related CM voltage and can generate large CM flux density and even cause core saturation. As shown in Fig. 1, the 3rd and 9th and higher order of fundamental frequency harmonics exist in the CM current spectrum when the central aligned continuous space vector modulation is used. The connecting AC and DC side midpoint EMI filter topology is popular in three phase converters such as rectifiers [17] - [18] and inverters [19]. Fig. 3(a) shows a connecting AC and DC midpoint with a capacitor C_{FB} structure in DC-fed motor drives. The capacitor C_{FB} provides a low impedance for high frequency CM noise and limits the CM noise within the converter, thus suppressing both AC and DC side CM noise. However, C_{FB} also provides a path for modulation frequency related components. A large capacitor C_{FB} will lead to large modulation frequency related CM current, which may cause CM inductor core saturation. To keep the EMI noise reduction performance of capacitor C_{FB} and suppress the modulation frequency related third harmonic, a notch filter structure is proposed as shown in Fig. 3(b). The resonance frequency of the notch filter is designed at the third harmonic of the modulation frequency. Since the notch filter only provides a high impedance around its resonance point, high frequency EMI noise bypassed by C_{notch} will not be influenced. Also, the notch inductor L_{notch} is not in the main current conduction path and mainly conducts the third harmonic components. It is significantly lighter than conventional EMI inductors, especially in high power conversion systems.

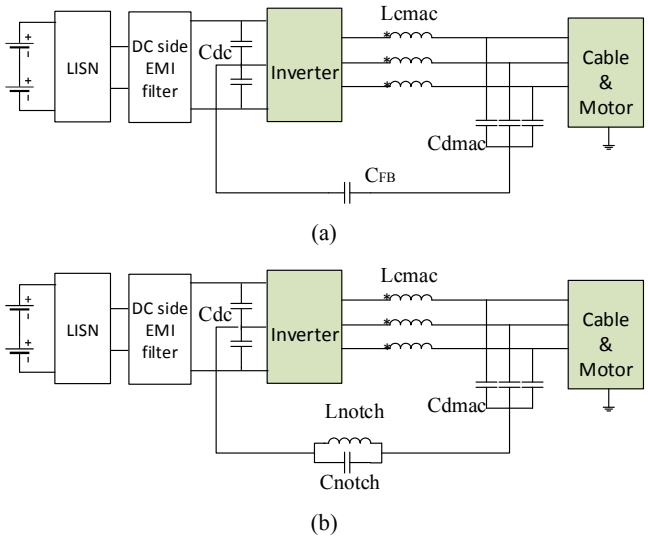

Fig. 3. (a) Connecting AC and DC midpoint CM filter structure in DC-fed motor drives. (b) Proposed notch filter structure.

Considering this analysis, in CM filter design, first the EMI bare noise should be investigated. The noise peaks which can probably determine CM filter corner frequency need to be analyzed and categorized. If the switching frequency related noise peak is very large, then a modulation method which reduces CM voltage magnitude can be considered. If system impedance resonance frequency related noise peak is dominant, then a damping network can be employed. Then, the CM filter is designed based on the updated noise attenuation requirement. After the CM filter is employed, system EMI noise and CM inductor current spectrum should be checked again to see if the CM filter introduces new resonances and if impedance resonance components and modulation frequency related components cause large CM flux density in the inductor core. If these components are large, then further damping and the proposed notch filter structure can be considered.

IV. EXPERIMENTAL VERIFICATION

A silicon carbide (SiC) device based three-phase neutral point clamped (ANPC) inverter is developed to verify the proposed concept and method. The switching frequency is 280 *kHz* and inverter AC output fundamental frequency is 3 *kHz*.

To reduce the switching frequency related CM voltage, the common-mode reduction (CMR) modulation scheme is employed. Fig. 4 shows the CM voltage spectrum comparison. Compared to conventional SVPWM, the CM voltage peak at switching frequency point reduced by a factor of 2 using CMR scheme, thus switching frequency related CM flux density will be reduced.

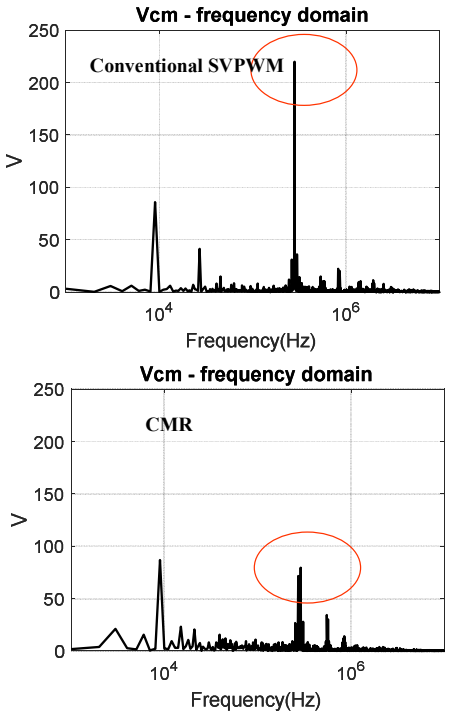

Fig. 4. CM voltage spectrum comparison: conventional SVPWM scheme versus CMR scheme.

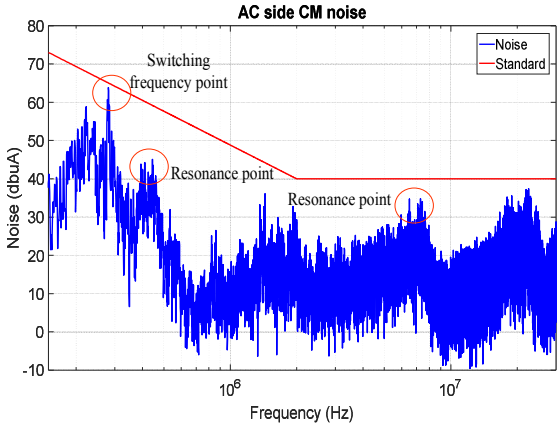

Fig. 5. EMI CM noise spectrum with impedance resonances well damped.

To reduce impedance resonance frequency related CM flux density components, the filter design concept and Rd-Cd damping networks discussed above are employed. Fig. 5 shows the CM noise current spectrum versus DO-160 EMI standard limit for aircraft application. All LC filters and load impedance resonance points are identified and well damped as shown in Fig. 5. The detailed filter and damping network parameters are not presented here for simplification. With this design, CM noise current and impedance resonance related CM flux density are not amplified and are quite small. The main LC filter parameters are designed based on the switching frequency noise peak attenuation requirement instead of the resonance peak to optimize inductor design.

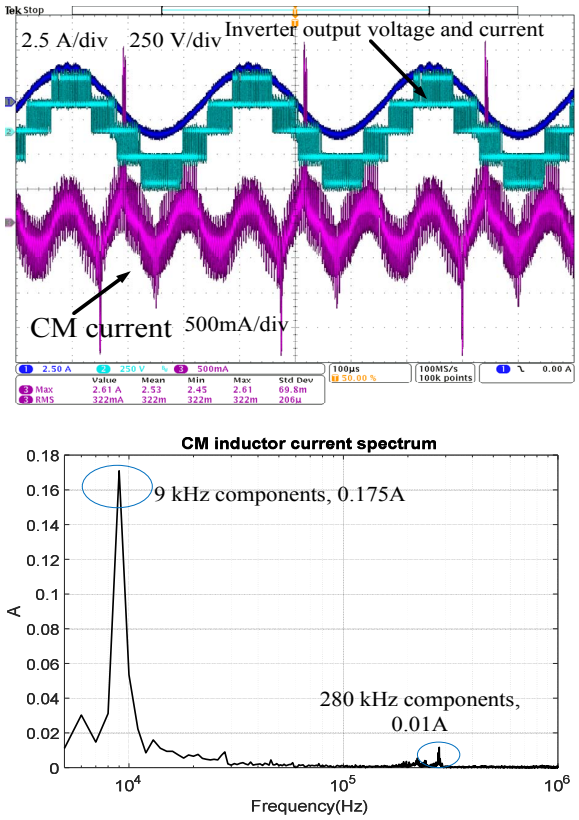

Fig. 6. Time domain waveform and related CM inductor CM current spectrum: with capacitor C_{FB}.

To reduce modulation frequency related components, the proposed notch filter structure in Fig. 3(b) is employed. SVM scheme is used to improve DC voltage utilization, the main modulation frequency related component is the third harmonic, which is 9 kHz in the experiment. Fig. 6 shows the comparison experiment results with only capacitor C_{FB} and with a notch filter (L_{notch} and C_{notch}). The capacitor values of the two cases are set to be the same, C_{FB}=C_{notch}=100 *nF*. To suppress the third harmonic, a notch inductor is determined as L_{notch}=3.3 *mH*. Fig. 6 shows the time domain waveform and related CM current spectrum using only C_{FB} . Large CM current distortion can be observed and the current spike exceeds 2.6 A when only

C_{FB} is used. This is because CM inductor is locally saturated due to large CM current while the third harmonic is the dominant component causing core saturation according to the current spectrum in Fig. 6. The time domain waveform and related CM current spectrum using a notch filter is shown in Fig. 7. CM current is significantly reduced and no current spike is observed. CM inductor will not be saturated. From the CM current spectrum, the 9 *kHz* third harmonic current is reduced by 3.75 times compared to the case using a capacitor.

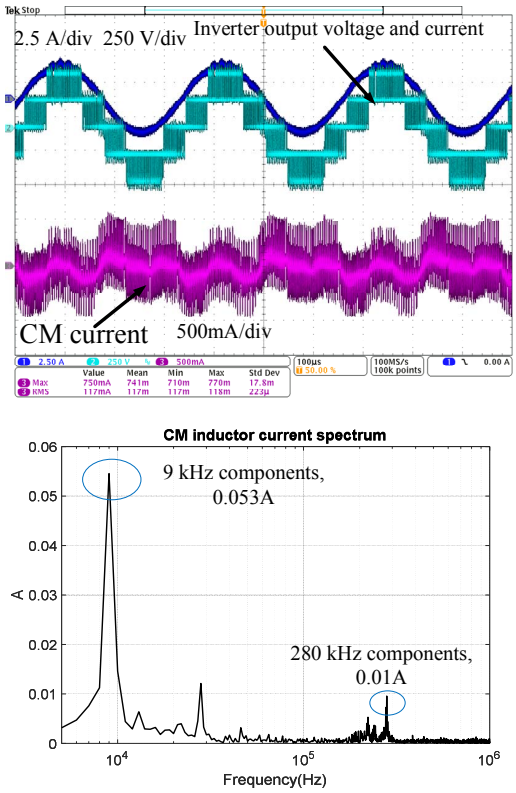

Fig. 7. Time domain waveform and related CM inductor CM current spectrum: with notch filter.

V. CONCLUSION

This paper introduces the spectrum concept for CM inductor core saturation analysis and design optimization. Both core permeability and modulation index have an opposite influence on DM and CM flux density. Thus, different core materials instead of a higher permeability core and converter worst operating condition for core flux density instead of full power case should be considered for CM EMI filter design. The switching frequency related components, impedance resonance frequency related components and modulation frequency related components are identified as the three main factors which can cause large CM flux density and saturation. Detailed CM flux density analysis and CM inductor design optimization are illustrated. Experiment results shows that, with the optimized design, switching frequency related CM voltage components and impedance resonance components are significantly reduced, and the proposed notch filter structure reduced the modulation frequency related components by 3.75 times and avoided the CM inductor core saturation.

ACKNOWLEDGMENT

The authors would like to thank The Boeing Company and NASA for their support of this research work. This work made use of the Engineering Research Center Shared Facilities supported by the Engineering Research Center Program of the National Science Foundation and DOE under NSF Award Number EEC-1041877 and the CURENT Industry Partnership Program.

REFERENCES

[1] W. Shen, F. Wang, D. Broyevich, V. Stefanovic, and M. Arpilliere, "Optimizing EMI filter design for motor drives considering filter component high-frequency characteristics and noise source impedance," *IEEE Applied Power Electronics Conference and Exposition (APEC)*, pp. 669-674, 2004.

[2] H. Chen, Z. Qian, S. Yang, and C. Wolf, "Finite-element modeling of saturation effect excited by differential-mode current in a common-mode choke," *IEEE Trans. Power Electron*., vol. 24, no. 3, pp. 873–877, Mar. 2009.

[3] R. Anne, B. Hans, D. Zhao, B. Ferreira, and L. Frank, "A new behavioral model for performance evaluation of common mode chokes," in *Proc. 2007 Int. Zurich Symp. Electromagn. Compat*., pp. 501-504, 2007.

[4] F. Luo, S. Wang, F. Wang, D. Boroyevich, N. Gazel, Y. Kang, and A. C. Baisden, "Analysis of CM Volt-second influence on CM inductor saturation and design for input EMI filters in three-phase DC-fed motor drive systems," *IEEE Trans. Power Electron.*, vol. 25, no. 7, pp. 1905-1914, Jul. 2010.

[5] L. Ran, S. Gokani, J. Clare, K. J. Bradley, and C. Christopoulos, "Conducted electromagnetic emissions in induction motor drive systems. II. Frequency domain models," *IEEE Trans. Power Electron*., vol. 13, no. 4, pp. 768–776, Jul. 1998.

[6] H. Akagi and T. Oe, "A specific filter for eliminating high-frequency leakage current from the grounded heat sink in a motor drive with an active front end," *IEEE Trans. Power Electron*., vol. 23, no. 2, pp. 763–770, Mar. 2008.

[7] H. Akagi and T. Shimizu, "Attenuation of conducted EMI emissions from an inverter-driven motor," *IEEE Trans. Power Electron*., vol. 23, no. 1, pp. 282–290, Jan. 2008.

[8] M. J. Nave, "On modeling the common mode inductor," in *Proc. IEEE Int. Symp. Electromagn. Compat*., pp. 452–457, 1991.

[9] E. Un and A. M. Hava, "A near-state PWM method with reduced switching losses and reduced common-mode voltage for three-phase voltage source inverters," *IEEE Trans. Ind. Appl.*, vol. 45, no. 2, pp. 782-793, Mar./Apr. 2009.

[10] A. M. Hava, N. O. Cetin, and E. Un, "On the contribution of PWM methods to the common mode (leakage) current in conventional three-phase two-level inverters as applied to ac motor drives," in *Conf. Rec. IEEE IAS Annu. Meeting*, pp. 1-8, 2008.

[11] N. O. Cetin and A. M. Hava, "Interaction between the filter and PWM units in the sine filter configuration utilizing three-phase ac motor drives employing PWM inverters," *IEEE Energy Conversion Congress and Exposition (ECCE)*, pp. 2592-2599, 2010.

[12] X. Zhang, D. Boroyevich, R. Burgos, P. Mattavelli, and F. Wang, "Evaluation of alternative modulation schemes for three-level neutral-point-clamped three-phase inverters," *Energy Conversion Congress and Exposition (ECCE)*, pp. 2131-2138, 2013.

[13] D. Jiang, F. Wang, "Variable switching frequency PWM for three-phase converters based on current ripple prediction," *IEEE Trans. Power Electron*., vol. 28, no. 11, pp. 4951–4961, Nov. 2013.

[14] A. M. Trzynadlowski, K. Borisov, Y. Li, and L. Qin, "A novel random PWM technique with low computational overhead and constant sampling frequency for high-volume, low-cost applications," *IEEE Trans. Power Electron*., vol. 20, no. 1, pp. 116–122, Jan. 2005.

[15] F. Shih, D. Chen, Y. Wu, and Y. Chen, "A procedure for designing EMI filters for AC line applications," *IEEE Trans. Power Electron.*, vol. 11, no. 1, pp. 170–181, Jan. 1996.

[16] R. W. Erickson, "Optimal single resistors damping of input filters," *IEEE Applied Power Electronics Conference and Exposition (APEC)*, pp. 1073-1079, 1999.

[17] M. Hartmann, H. Ertl, and J. W. Kolar, "EMI filter design for a 1MHz, 10 kW three-phase/level PWM rectifiers," *IEEE Trans. Power Electron.*, vol. 26, no. 4, pp. 1192–1204, Apr. 2011.

[18] R. Chen, Y. Yao, L. Zhao and M. Xu, "Inhibiting mains current distortion for SWISS Rectifier – a three-phase buck-type harmonic current injection PFC converter," *IEEE Applied Power Electronics Conference and Exposition (APEC)*, pp. 1850-1854, 2015.

[19] X. Zhang, D. Boroyevich, P. Mattavelli, J. Xue, and F. Wang, "EMI filter design and optimization for both AC and DC side in a DC-fed motor drive system," *Applied Power Electronics Conference and Exposition (APEC)*, pp. 597-603, 2013.

[20] F. Luo, D. Dong, D. Boroyevich, P. Mattavelli, and S. Wang, "Improving high-frequency performance of an input common mode EMI filter using an impedance-mismatching filter," *IEEE Trans. Power Electron.*, vol. 29, no. 10, pp. 5111- 5115, Jul. 2014.

[21] J. Xue, F. Wang, X. Zhang, D. Broyevich, P. Mattavelli, "Design of output passive EMI filter in Dc-fd motor drive," *IEEE Applied Power Electronics Conference and Exposition (APEC)*, pp. 634-640, 2012.

[22] L. Xing, M. Shen, M. li and W. Said, "Common mode choke optimization for three-phase motor drive systems," *IEEE Energy Conversion Congress and Exposition (ECCE)*, pp. 1399-1405, 2012.